

## Nanopod Formation through Gold Nanoparticle Templated and Catalyzed Cross-linking of Polymers Bearing Pendant Propargyl Ethers

Ke Zhang,<sup>†</sup> Joshua I. Cutler,<sup>†</sup> Jian Zhang, Dan Zheng, Evelyn Auyeung, and Chad A. Mirkin\*

Department of Chemistry and International Institute for Nanotechnology, Northwestern University, 2145 Sheridan Road, Evanston, Illinois 60208-3113

Received August 11, 2010; E-mail: chadnano@northwestern.edu

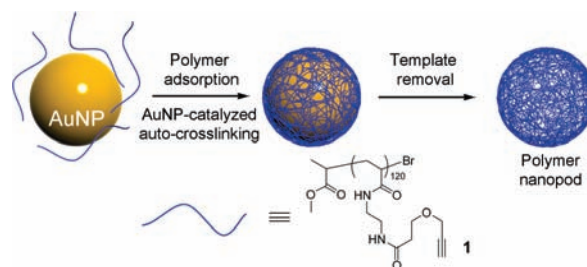
**Abstract:** A novel method for synthesizing polymer nanopods from a linear polymer bearing pendant propargyl ether groups, using gold nanoparticles as both the template and the catalyst for the cross-linking reaction, is reported. The transformations involved in the cross-linking process are unprecedented on the surface of a gold particle. A tentative cross-linking mechanism is proposed.

Hollow nanostructures have attracted significant interest in recent years due to their unique chemical, physical, and biological properties, which suggest a wide range of applications in drug/gene delivery,<sup>1–3</sup> imaging,<sup>4,5</sup> and catalysis.<sup>6</sup> Accordingly, a variety of methods have been developed to synthesize these structures based upon emulsion polymerization,<sup>7–9</sup> layer-by-layer processes,<sup>10</sup> cross-linking of micelles,<sup>11–13</sup> molecular or nanoparticle self-assembly,<sup>14,15</sup> and sacrificial template techniques.<sup>16–19</sup> Among them, the templating method is particularly powerful in that it transfers the ability to control the size and shape of the template to the product, for which desired homogeneity and morphology can be otherwise difficult to achieve. In a typical templated synthesis, a sacrificial core is chosen, upon which preferred materials containing latent cross-linking moieties are coated. Following the stabilization of the coating through chemical cross-linking, the template is removed, leaving the desired hollow nanoparticle. This additional cross-linking step can be easily achieved for compositionally simple molecules, such as poly(acrylic acid) or chitosan.<sup>20,21</sup> However, for systems containing sensitive and/or biologically functional structures, conventional cross-linking chemistries may not be sufficiently orthogonal to prevent the loss of their activity.

In this report, we disclose a method for synthesizing polymer nanopods from a linear polymer bearing pendant propargyl ether groups (**1**), utilizing gold nanoparticles (AuNPs) as both the template for the formation of the shell and the catalyst for the cross-linking reaction (Scheme 1). No additional cross-linking reagents or synthetic operations are required. This novel reaction is both fundamentally interesting and technologically useful. Indeed, it appears to be the first example of AuNP-catalyzed cross-linking of alkyne-based adsorbates and yields well-defined, homogeneous hollow nanostructures.

Au(I) and Au(III) ions and their complexes display remarkable alkyneophilicity and have been increasingly recognized as potent catalysts for organic transformations.<sup>22–25</sup> Recently, it has been demonstrated that Au(0) surfaces also adsorb terminal alkyne groups and form relatively densely packed and stable monolayers.<sup>26</sup> However, the type of interaction that exists between the alkyne and the gold surface is not well understood. Moreover, it is not

**Scheme 1.** Synthesis of Polyvalent Propargyl Ether Nanopods



clear whether such interaction makes the alkyne group more susceptible to chemical reactions, such as nucleophilic additions typically observed with ionic gold–alkyne complexes. Bearing multiple side arm propargyl ether groups, polymer **1** readily adsorbs onto citrate-stabilized 13 nm AuNPs prepared in an aqueous solution following the Turkevich–Frens method.<sup>27,28</sup> X-ray photoelectron spectroscopy (XPS) confirmed the adsorption of the polymer onto AuNPs (Figure S1-A). Excess polymer was removed by iterative centrifugation and subsequent resuspension steps. The resulting polymer-coated AuNPs exhibit a plasmon resonance at 524 nm, characteristic of dispersed particles, and there is no evidence of aggregation even after 8 weeks of storage at room temperature. Therefore, even though **1** is a potential interparticle cross-linking agent, it does not lead to aggregation of the AuNPs, a conclusion that is corroborated by Dynamic Light Scattering (DLS, Figure S2) and electron microscopy (*vide infra*).

To determine the surface polymer density, we designed a fluorescence-based titration assay utilizing Alexa Fluor (AF) 488-labeled polymer **1**, prepared *via* click chemistry. Because AuNPs can serve as fluorescence quenchers, when increasing amounts of polymer are added, fluorescence intensities increase at a slower rate while the AuNP surface is being initially covered, and then at a much higher rate thereafter. The onset of the second stage indicates the point at which full coverage has occurred (Figure S3). For 13 nm AuNPs, it is determined that on average 26.0 polymer chains can adsorb onto each particle, which gives a surface density of 2.27 mg·m<sup>-2</sup>. For 30 nm AuNPs, 128.3 polymer chains can adsorb onto each particle. The polymer surface density, however, is nearly identical to that determined for the 13 nm AuNPs (2.32 mg·m<sup>-2</sup>).

Dissolution of the AuNP core was achieved using potassium cyanide (KCN) in the presence of oxygen. When KCN is added to unmodified citrate-capped AuNPs, the color of the solution instantly changes from red to purple, a consequence of colloid destabilization and particle aggregation.<sup>29</sup> However, for the polymer-coated AuNPs, the color remains red throughout the dissolution process, only decreasing in intensity until the solution is colorless (Figure 1A). Time dependent UV–vis spectra show a gradual blue shift of

<sup>†</sup> These authors contributed equally.

the plasmon resonance maximum from 524 to 515 nm (Figure 1B), as expected from the decrease in AuNP size.<sup>30</sup> The dissolution process also can be visualized by Transmission Electron Microscopy (TEM) (Figure 1C). As the outer layer of the AuNP was oxidatively dissolved, a gray, uranyl acetate-stained shell could be observed. Complete removal of the template affords nanopods that retain the size of their template with high fidelity. When AuNPs of increasing size were used (13, 20, 30, and 40 nm), the resulting nanopods reflected the size of the NP templates, as determined by DLS and TEM (Figure 2).

These observations lead us to conclude that **1** has formed a cross-linked shell around the AuNPs, thereby preventing the partially dissolved AuNPs from escaping and aggregating. In this process, the AuNP not only templates the formation of the shell but also

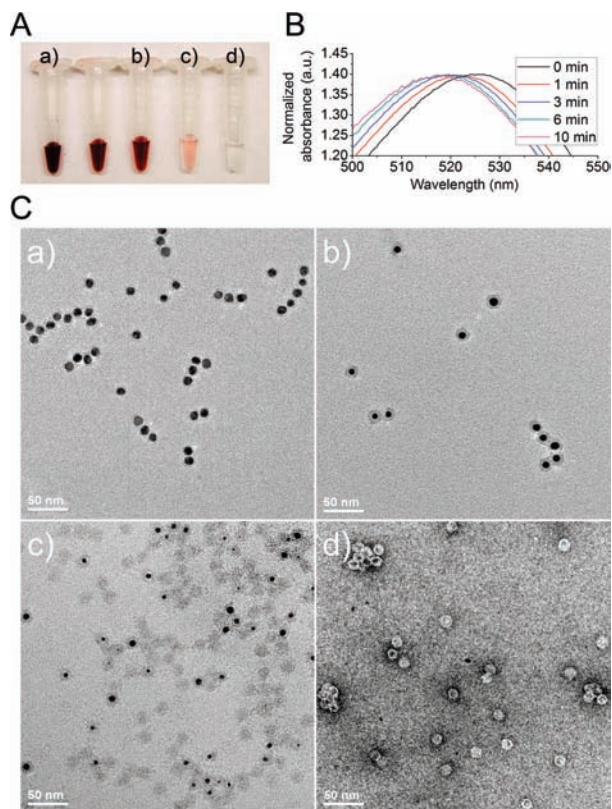


**Figure 1.** (A) Dissolution process of polymer-coated 13 nm AuNPs. (B) Normalized UV-vis spectra of AuNPs at various time points during the dissolution process. (C) TEM images of (a) polymer-coated AuNPs, (b–c) partially formed nanopods, and (d) fully formed nanopods (negatively stained with 0.5% uranyl acetate).

catalyzes the cross-linking reaction. This convenient synthesis of nanopods could in principle open up a new avenue to a broad range of functional nanostructures.

However, the microscopy experiments do not provide an understanding of the chemistry that underlies the formation of the nanopods. To probe this issue more deeply, we followed the reaction on the particle surface by IR and NMR spectroscopy and with model ligands and complexes. IR spectroscopy of **1** before and after cross-linking on the surface of the 13 nm AuNP shows the complete loss of alkyne  $\text{C}\equiv\text{C}$  stretching ( $2114\text{ cm}^{-1}$ ),  $\text{C}-\text{H}$  stretching ( $3805\text{ cm}^{-1}$ ), and  $\text{C}-\text{H}$  bending ( $1274, 646\text{ cm}^{-1}$ ) modes, indicating that the propargyl ether group is directly involved in the reaction (Figure S4-D). NMR spectroscopy of the nanopods made from 13 nm AuNPs proved difficult due to low sensitivity, line broadening, and extensive signal overlap. However, 5 nm AuNPs yield nanopods

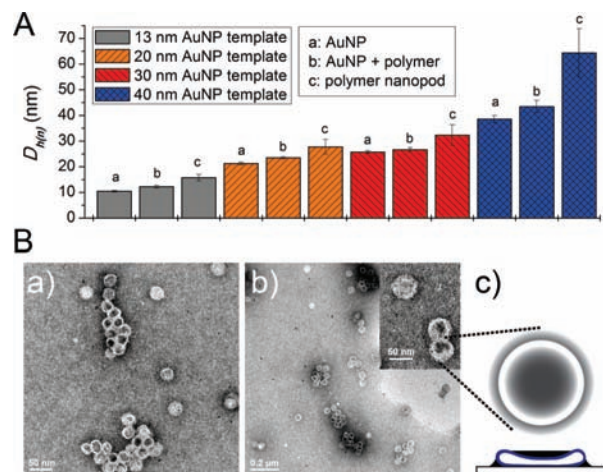


**Figure 2.** (A) Number-average hydrodynamic diameters of AuNPs (13, 20, 30, and 40 nm), polymer-coated AuNPs, and polymer nanopods. (B) TEM images of (a) 20 nm nanopods and (b) 40 nm nanopods (negatively stained with 0.5% uranyl acetate). In (c) it is illustrated why nanopods appear as donut-shaped in TEM. Black: uranyl acetate stain. Blue: deflated nanopod on a surface.

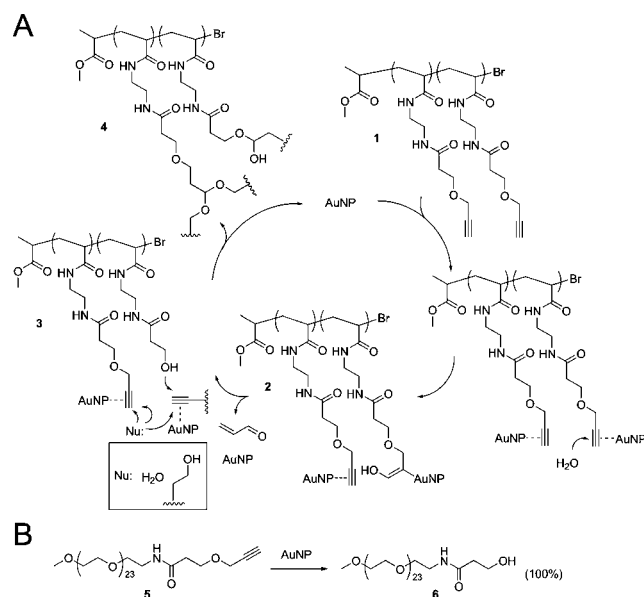


**Figure 3.** (A) Tentative cross-linking mechanism. (B) A poly(ethylene glycol)<sub>24</sub>-propargyl ether conjugate model system.

sufficiently small to be analyzed.  $^1\text{H}$  and  $^{13}\text{C}$  NMR spectroscopy showed the loss of resonances from the propargyl group, which likely occurs *via* elimination of acrylaldehyde to form a hydroxyl group.<sup>31</sup> The resulting hydroxyl group then serves as a new nucleophile for remaining alkyne–Au complexes to generate acetal linkages.<sup>32</sup> Indeed, the  $^1\text{H}-^{13}\text{C}$  HSQC spectrum shows the appearance of resonances indicative of the  $\alpha$ -H of a primary alcohol ( $\delta$  3.81 ppm,  $^1\text{H}$ ), an alkyl ether ( $\delta$  3.74 ppm,  $^1\text{H}$ ), and an acetal ( $\delta$  4.32 ppm,  $^1\text{H}$ ) group (Figure S4-B and S4-C). Moreover, the C1s peak in the XPS of the polymer–gold complex exhibits a shoulder at 291.3 eV, consistent with the presence of an acetal carbon and our proposed mechanism (Figure S1-B). Such transformations are previously known to be possible only with ionic gold catalysts. Although a detailed mechanism of the present protocol awaits further studies, a plausible pathway can be advanced (Figure 3A). Coordination of the alkynophilic AuNP to **1** is followed by the nucleophilic addition of water to yield intermediate **2**, which

forms **3** by elimination. Because of high local concentrations on the surface of the AuNP, reaction between the hydroxyl groups and Au–alkyne complexes is possible without high temperatures, giving acetal and ether cross-links **4** and regenerating the catalyst AuNP. However, the AuNP cannot catalyze further reactions because the dense shell that forms prevents it from accessing free polymers. Indeed, we found that the free polymers separated from the reaction mixtures were exclusively the starting material **1**.

To gain further insight into the proposed mechanism, we synthesized a monodisperse poly(ethylene glycol)<sub>24</sub>-propargyl ether conjugate **5**, which allowed for convenient mass and NMR analyses (Figure 3B). Because **5** contains only one propargyl ether moiety, once it loses the gold-binding alkyne group, it can no longer bind to the AuNP surface, thereby exposing the AuNP surface to catalyze further reactions. Indeed, upon incubation with AuNPs and subsequent removal of AuNPs through centrifugation, **5** was converted to the primary alcohol **6** quantitatively as evidenced by matrix-assisted laser desorption/ionization time-of-flight mass spectrometry (MALDI-ToF MS) and NMR spectroscopy (Figure S5). This is in contrast to the polymer system, wherein only the polymers associated with the AuNPs were subject to catalysis due to the irreversible formation of a dense shell. These results are consistent with the conclusion that the AuNP is the catalyst for the chemical transformations (*vide supra*).

In summary, we have demonstrated a novel method for synthesizing well-defined polymer nanopods from a linear polymer with pendant propargyl ether groups, using a AuNP as the template and the catalyst for the cross-linking reaction. The size of the nanopods can be controlled by choosing different AuNP templates. We envisage that this general strategy can be applied to create a variety of complex and functional systems that are applicable in a broad range of disciplines.

**Acknowledgment.** We thank the NCI-CCNE program, the DOE Office (Award No. DE-SC0000989) for support via the NU Non-equilibrium Energy Research Center, and the NSF-NSEC program for financial support. Electron microscopy was performed in the EPIC facility of the NUANCE center at Northwestern University.

**Supporting Information Available:** Experimental procedures and characterization data. This materials is available free of charge via the Internet at <http://pubs.acs.org>.

## References

- (1) Shu, S.; Zhang, X.; Wu, Z.; Wang, Z.; Li, C. *Biomaterials* **2010**, *31*, 6039.
- (2) Kim, E.; Kim, D.; Jung, H.; Lee, J.; Paul, S.; Selvapalam, N.; Yang, Y.; Lim, N.; Park, C. G.; Kim, K. *Angew. Chem., Int. Ed.* **2010**, *49*, 4405.
- (3) Kasuya, T.; Jung, J.; Kinoshita, R.; Goh, Y.; Matsuzaki, T.; Iijima, M.; Yoshimoto, N.; Tanizawa, K.; Kuroda, S. i. In *Methods in Enzymology*; Nejat, D., Ed.; Academic Press: 2009; Vol. 464, p 147.
- (4) Sharma, S.; Paiphansiri, U.; Hombach, V.; Mailänder, V.; Zimmermann, O.; Landfester, K.; Rasche, V. *Contrast Media Mol. Imaging* **2010**, *5*, 59.
- (5) Tan, H.; Liu, N. S.; He, B.; Wong, S. Y.; Chen, Z.-K.; Li, X.; Wang, J. *Chem. Commun.* **2009**, 6240.
- (6) Choi, S.-H.; Gopalan, A. I.; Ryu, J.-H.; Lee, K.-P. *Mater. Chem. Phys.* **2010**, *120*, 18.
- (7) Anton, N.; Benoit, J.-P.; Saulnier, P. *J. Controlled Release* **2008**, *128*, 185.
- (8) Landfester, K.; Musyanovych, A.; Mailänder, V. *J. Polym. Sci., Part A: Polym. Chem.* **2010**, *48*, 493.
- (9) Li, W.; Yoon, J. A.; Matyjaszewski, K. *J. Am. Chem. Soc.* **2010**, *132*, 7823.
- (10) Kondo, K.; Kida, T.; Ogawa, Y.; Arikawa, Y.; Akashi, M. *J. Am. Chem. Soc.* **2010**, *132*, 8236.
- (11) Turner, J. L.; Wooley, K. L. *Nano Lett.* **2004**, *4*, 683.
- (12) Sugihara, S.; Armes, S. P.; Lewis, A. L. *Angew. Chem., Int. Ed.* **2010**, *49*, 3500.
- (13) Moughton, A. O.; Stubenrauch, K.; O'Reilly, R. K. *Soft Matter* **2009**, *5*, 2361.
- (14) Kim, D.; Kim, E.; Kim, J.; Park, K. M.; Baek, K.; Jung, M.; Ko, Y. H.; Sung, W.; Kim, H. S.; Suh, J. H.; Park, C. G.; Na, O. S.; Lee, D.-k.; Lee, K. E.; Han, S. S.; Kim, K. *Angew. Chem., Int. Ed.* **2007**, *46*, 3471.
- (15) Kim, D.; Kim, E.; Lee, J.; Hong, S.; Sung, W.; Lim, N.; Park, C. G.; Kim, K. *J. Am. Chem. Soc.* **2010**, *132*, 9908.
- (16) Réthoré, G.; Pandit, A. *Small* **2010**, *6*, 488.
- (17) Marinakos, S. M.; Novak, J. P.; Brousseau, L. C.; House, A. B.; Edeki, E. M.; Feldhaus, J. C.; Feldheim, D. L. *J. Am. Chem. Soc.* **1999**, *121*, 8518.
- (18) Caruso, F.; Caruso, R. A.; Möhwald, H. *Science* **1998**, *282*, 1111.
- (19) Liz-Marzán, L. M.; Giersig, M.; Mulvaney, P. *Langmuir* **1996**, *12*, 4329.
- (20) Cheng, C.; Qi, K.; Khoshdel, E.; Wooley, K. L. *J. Am. Chem. Soc.* **2006**, *128*, 6808.
- (21) Hu, Y.; Ding, Y.; Ding, D.; Sun, M.; Zhang, L.; Jiang, X.; Yang, C. *Biomacromolecules* **2007**, *8*, 1069.
- (22) Hashmi, A. S. K. *Chem. Rev.* **2007**, *107*, 3180.
- (23) Li, Z.; Brouwer, C.; He, C. *Chem. Rev.* **2008**, *108*, 3239.
- (24) Fürstner, A.; Davies, P. W. *Angew. Chem., Int. Ed.* **2007**, *46*, 3410.
- (25) Hashmi, A. S. K.; Hutchings, G. J. *Angew. Chem., Int. Ed.* **2006**, *45*, 7896.
- (26) Zhang, S.; Chandra, K. L.; Gorman, C. B. *J. Am. Chem. Soc.* **2006**, *129*, 4876.
- (27) Frens, G. *Colloid Polym. Sci.* **1972**, *250*, 736.
- (28) Turkevich, J.; Stevenson, P. C.; Hillier, J. *Discuss. Faraday Soc.* **1951**, *11*, 55.
- (29) Daniel, M.-C.; Astruc, D. *Chem. Rev.* **2003**, *104*, 293.
- (30) Link, S.; El-Sayed, M. A. *J. Phys. Chem. B* **1999**, *103*, 4212.
- (31) Fukuda, Y.; Utimoto, K. *Bull. Chem. Soc. Jpn.* **1991**, *64*, 2013.
- (32) Fukuda, Y.; Utimoto, K. *J. Org. Chem.* **1991**, *56*, 3729.

JA107224S